Atmos. Chem. Phys. Discuss., 9, 13355–13406, 2009
www.atmos-chem-phys-discuss.net/9/13355/2009/

Atmospheric Chemistry and Physics Discussions

This discussion paper is/has been under review for the journal *Atmospheric Chemistry and Physics (ACP)*. Please refer to the corresponding final paper in *ACP* if available.

A photochemical model and sensitivity study of the triple-oxygen isotopic ($\Delta^{17}O$) composition of NO_y , HO_x, and H_2O_2 in a polluted boundary layer

G. Dominguez[1], G. Wilkins[1,2], and M. H. Thiemens[1]

[1]University of California, San Diego, Department of Chemistry and Biochemistry, La Jolla, California, USA
[2]University of California, Berkeley, Department of Mathematics, Berkeley, California, USA

Received: 22 May 2009 – Accepted: 26 May 2009 – Published: 17 June 2009

Correspondence to: G. Dominguez (gdominguez@ucsd.edu)

Published by Copernicus Publications on behalf of the European Geosciences Union.

Abstract

We present a photochemical model developed for the *explicit* calculation of triple oxygen isotopic compositions ($\Delta^{17}O$) of major atmospheric species. While we focus on the $\Delta^{17}O$ of HNO_3 and aerosol nitrate (NO_3^-) and its precursors such as NO, NO_2 and N_2O_5, the general implementation given here also provides $\Delta^{17}O$ predictions for other important atmospheric compounds such as OH, H_2O_2, and HO_2. Through the use of a simple aerosol surface area model, we calculate the $\Delta^{17}O$ composition of aerosol nitrate produced as a function of aerosol size and aerosol surface type. We explore the sensitivity of the $\Delta^{17}O$ of atmospheric species through a series of sensitivity studies and show that the $\Delta^{17}O$ of atmospheric compounds is affected to various degrees by environmental factors such as temperature, relative humidity, ozone concentration, NO_x flux, and total ozone column density. In addition, we find that $\Delta^{17}O$ of these species is sensitive to photochemical conditions such as cloud albedo, latitude, and time of year. We compare the $\Delta^{17}O$ calculation outputs to previous methods and find significant differences in the $\Delta^{17}O$ of NO_2. We describe the origins of these and suggest studies that may help to resolve these differences.

1 Introduction: triple oxygen isotopic composition of atmospheric species

Oxygen has three stable isotopes (^{16}O,^{17}O, ^{18}O) and until 1974, it was believed that all measurements of oxygen bearing species on Earth had a well defined relationship between their $\frac{[^{17}O]}{[^{16}O]}$ and $\frac{[^{18}O]}{[^{16}O]}$ ratios. Conventionally, the isotopic content of ^{17}O and ^{18}O are expressed as ratios with respect to a standard and quantified as $\delta^{18}O$ and $\delta^{17}O$ (see Appendix A) and when plotted on a so-called triple-isotope plot ($\delta^{17}O$ vs. $\delta^{18}O$), these ratios typically fall along a line with slope approximately equal to 0.52. This slope results from the fact that most physical processes that enrich or deplete the isotopic content of a system do so as a function mass and the relative depletion or enrichment

ACPD

9, 13355–13406, 2009

of isotopes of a given element in compounds is determined by the mass differences between the isotopes (see Thiemens, 2006). Thus, for most oxygen bearing terrestrial compounds, knowledge of $\delta^{18}O$ is sufficient for knowing $\delta^{17}O$, since these are related by $\delta^{17}O \simeq 0.52 \times \delta^{18}O$ when referenced to the Standard Mean Ocean Water (SMOW) standard.

The discovery that ozone (O_3) produced in the lab (Thiemens and Heidenreich, 1983) and in the atmosphere (Mauersberger, 1986; Johnston and Thiemens, 1997) is anomalously enriched in ^{17}O has led to novel applications in the use of both $\delta^{18}O$ and $\delta^{17}O$ in measurements atmospheric compounds, where O_3 is a major oxidant. The anomalous enrichment in ^{17}O , is transferred to both the direct and indirect products of ozone oxidation. For the purposes of this paper, this excess (or deficit) of ^{17}O is quantified as:

$$\Delta^{17}O \simeq \delta^{17}O - (0.52)\delta^{18}O \quad (1)$$

Most solid and liquid oxygen bearing compounds found on Earth have $\Delta^{17}O \simeq 0‰$.

In recent years atmospheric compounds that have been identified as having ^{17}O excesses or deficits ($\Delta^{17}O \neq 0$) include CO (Huff and Thiemens, 1998; Rockmann et al., 1998), CO_2 (Thiemens et al., 1991), N_2O (Cliff and Thiemens, 1997), H_2O_2 (Savarino and Thiemens, 1999a), perchlortate (Bao and Gu, 2004), molecular oxygen (Luz and Barkan, 2005), nitrate (NO_3^-) (Michalski et al., 2003) and sulfate (SO_4^{2-}) (Bao et al., 2000a,b; Lee and Thiemens, 2001; Bao et al., 2008). Most of these compounds acquire their anomalous enrichments either directly or indirectly from ozone, and measurements of the triple-oxygen isotopic composition ($\Delta^{17}O$) of these species, when combined with a detailed understanding of how the ^{17}O anomalies are transferred, can be used to gain direct measurements of the relative contribution of important chemical pathways. Aerosol nitrate (Morin et al., 2008; Kunasek et al., 2008; Morin et al., 2007a; Patris et al., 2007) and sulfate (Alexander et al., 2009; Bao et al., 2008; Dominguez et al., 2008), in particular, have been studied most extensively through a combination of measurements and modeling. For the purpose of illustrating some of

the novel constraints that can be provided through isotopic measurements of atmospheric compounds, in particular that of nitrate, as well as to provide additional context for understanding the motivation and significance of the work we present, we briefly previous measurements and modeling of $\Delta^{17}O$ of NO_y(=NO, NO_2, HNO_3, and NO_3^-) and HO_x(=OH, HO_2) in this next section.

1.1 Recent work on $\Delta^{17}O$ of tropospheric nitrate and its precursors

The $\Delta^{17}O$ values of aerosol nitrate found in a variety of environments have been published recently. Michalski et al. (2003) first measured and modeled the $\Delta^{17}O$ bulk isotopic composition of aerosol nitrate in a polluted boundary layer using outputs of the photochemical model developed by Yvon et al. (1996). The photochemical model used by these authors included a two-stream radiative transfer model and could take inputs that included temperature, relative humidity (RH), total ozone column (TOC), NO_x flux, and ozone concentrations. NO_x and ozone concentrations could be held constant in the model, thus explicit treatment of ozone production was not included. By assuming a constant $\Delta^{17}O$ for ozone (=35‰) and determining the relative contribution of various oxidation pathways for NO and NO_2, precursors of aerosol nitrate, the authors found that the isotopic composition of aerosol nitrate has a seasonal variability attributed to shifts in temperature and actinic flux. Because the work done by Michalski et al. (2003) focused on the bulk isotopic composition of aerosol nitrate, the model predictions did not have any size dependent chemistry. Nevertheless, the authors, in general, found good agreement between their observations of the bulk isotopic composition of aerosol nitrate and their model results, although some significant differences between the model and measurements were reported. The authors attributed these differences to the possible influence of transport.

Since then, several studies of $\Delta^{17}O$ in aerosol nitrate from a variety of environments have been published. Patris et al. (2007) measured the size-dependent values of $\Delta^{17}O$ in nitrate (and sulfate) in a remote boundary layer (Trinidad Head, CA, USA) and found modest, but statistically significant differences in the $\Delta^{17}O$ values of aerosol nitrate as

a function of aerosol size, with the coarse size fraction displaying systematically higher values (0.5–1.5‰). This systematic difference was attributed to the preferential uptake of N_2O_5 on coarse aerosol particles, although this process was not modeled by the authors. Morin et al. (2007a) studied the shift in $\Delta^{17}O$ of aerosol nitrate at a coastal Arctic site and found direct evidence supporting the expectation that the concentration of ozone directly affects the $\Delta^{17}O$ found in aerosol nitrate. In addition, the authors argued for the importance of BrO as an oxidant of NO_2 to explain their comparatively high $\Delta^{17}O(NO_3^-)$ (≃35‰) in the Arctic environment. Morin et al. (2007a) did not model their observations, and instead relied upon the use of analytical approximations to illustrate the need for the BrO oxidation channel to explain their isotopic data.

In an effort to better understand the variability of $\Delta^{17}O$ of ice-core nitrate from Alexander et al. (2004) and its relationship to paleoclimate concentrations of O_3 and OH, Kunasek et al. (2008) measured $\Delta^{17}O$ of snowpit nitrate and compared these measurements to the outputs of a box-model of atmospheric nitrate for over three seasons. The authors found values of a seasonal variations in $\Delta^{17}O$ that ranged from ~22‰ (summer) to 33.7‰ (winter). The authors modeled their data using the combination of a chemical box model (which did not include Br chemistry) supplemented with boundary conditions set by the output of the GEOS-Chem transport model(Park et al., 2004). In a manner similar to the treatment of Michalski et al. (2003), the authors calculated the $\Delta^{17}O$ values of NO_2 and nitrate using the computed chemical production rates output from their box model. Interestingly, the authors found very good agreement between the results of their model and isotopic observations during the winter, but their model appears to underpredict the $\Delta^{17}O$ of snowpit nitrate by 2–7‰ during the summer, potentially caused by the combination of assuming that $\Delta^{17}O(OH)$=0‰, the subduction of stratospheric ozone (which has a higher ^{17}O anomaly), or the role of BrO in producing nitrate. Morin et al. (2008) measured and modeled the $\Delta^{17}O$ of aerosol nitrate over an annual cycle in the Arctic. For this work, the authors employed a 0D Lagrangian box model to track the chemistry along the trajectory followed by air transiting to the sampling site. Reasonable agreement between their model and measurements are

found, although there is significant scatter in the data beyond the analytical uncertainties. Similar to previous work, the $\Delta^{17}O$ of nitrate was estimated using the outputs of a chemistry model and several simplifying assumptions to estimate the $\Delta^{17}O$ of aerosol nitrate. The authors invoked BrO oxidation of NO to explain their isotopic measurements. Most recently, Alexander et al. (2009) have presented a global-transport model of $\Delta^{17}O$ of nitrate which uses a similar methods to calculate $\Delta^{17}O$ of nitrate.

To date, there appears to be some controversy regarding the precise value of $\Delta^{17}O(O_3)$ in the atmosphere and recent laboratory experiments on the distribution of oxygen isotopes within molecules of ozone (Bhattacharya et al., 2008) has called into question some of the model assumptions made by Michalski et al. (2003). Morin et al. (2007a), for example, argue that the *bulk* $\Delta^{17}O$ found in tropospheric O_3 is closer to the 25‰ found by Johnston and Thiemens (1997) and not the 35‰ assumed by Michalski et al. (2003) and Lyons (2001). However, the enrichment of ^{17}O in the terminal atom position of O_3 (Savarino et al., 2008) may explain the good agreement between the observations and modeling of Michalski et al. (2003).

2 Motivation for present work

Given the recent increases and applications of triple-oxygen isotopic measurements in the environment, from tropical rain forests (Brothers et al., 2008) to polluted marine boundary layers (Dominguez et al., 2008), it has become clear that a systematic study of the sensitivity of $\Delta^{17}O$ of atmospheric species is needed in order to maximize the potential of $\Delta^{17}O$ measurements to provide unique and novel insights into atmospheric chemistry that are not possible using traditional concentration measurements. In this paper, we present a photochemical box model that *explicitly* calculates the $\Delta^{17}O$ composition of major oxygen bearing species as a function of various oxidative and photochemical conditions. While the primary driver of the present work is to better understand observations of aerosol nitrate in the environment, we also calculate the $\Delta^{17}O$ of important precursor molecules of aerosol nitrate such as NO_2, HO_2, NO_3,

and N_2O_5. As a consequence, we provide the first direct calculations of the $\Delta^{17}O$ of HO_x and H_2O_2 in the atmosphere as a function of various environmental variables.

There are several benefits and drawbacks that accompany the explicit approach taken here. First, by not resorting to approximations that simplify the analytical calculation of $\Delta^{17}O$ of species, we avoid overlooking small contributions by precursors that may have an overall cumulative effect on $\Delta^{17}O$. In addition, this approach allows us to examine the effect of shorttime scale perturbations on the photochemical and oxidative conditions at a sampling site or in studies of plume photochemistry that are not possible with previous modeling approaches. The lack of transport, on the other hand, is also a drawback of the box-model approach. Finally, we should mention that the explicit tracking of $\Delta^{17}O$ in atmospheric species, as will be described in Sect. 5.2, is computationally expensive, in essence adding an additional chemical species for each one whose $\Delta^{17}O$ is tracked in the photochemical model. The benefits of our explicit $\Delta^{17}O$ approach, in the end, have allowed us to identify a potentially significant oversimplification of previous work regarding the $\Delta^{17}O$ of HO_2, a significant oxidant and precursor to nitrate in the atmosphere.

3 Overview of present work

This paper is organized as follows. First, we review the mechanisms of ^{17}O anomaly transfer in the atmosphere using the NO_x-O_3 system as an example. We then provide a brief overview of the isotopic photochemical box model developed and include a description of key modifications made to the precursor code such as the inclusion of aerosol and isotopic sub-models that directly tracks the propagation of $\Delta^{17}O$ from O_3 to other other major oxygen bearing species in the atmosphere as a function of time. Using this model, we calculate the instantaneous and time-averaged values of $\Delta^{17}O$ for a variety key oxygen bearing species in the troposphere. We should emphasize that this work, while similar in some aspects to previous modeling work reviewed in the previous section, is novel and significant. As we will show, our approach has allowed us

to identify an important consideration in the calculation of $\Delta^{17}O$ of tropospheric species that has been overlooked by previous work. The significance of this finding along with others is discussed in Sect. 8.

Before describing the photochemical model, we briefly review the mechanisms of anomalous ^{17}O transfer to atmospheric species, with particular emphasis on oxidized species of nitrogen, although the physical and photochemical processes described may apply to other species as well.

4 The origin of excess ^{17}O in atmospheric nitrate

Natural (e.g. lightning and biomass burning) and anthropogenic emissions (automobiles, powerplants, and biomass burning) of oxidized nitrogen (NO_x) eventually become fully oxidized in the atmosphere leading to the production of nitric acid (HNO_3), nitrous acid (HONO), the nitrate radical (NO_3), dinitrogen pentoxide (N_2O_5), peroxyacetyl nitrate (PAN,$CH_3C(O)OONO_2$), alkyl nitrates ($RONO_2$), and peroxyalkyl nitrates ($ROONO_2$). Nitric acid is the major product of the atmospheric oxidation of NO_x (Seinfeld and Pandis, 2006).

Recently, it was shown that the $\Delta^{17}O$ of aerosol nitrate found in the atmosphere can be quantified (Michalski et al., 2002) and that these measurements can be used to understand the relative role that homogeneous and heterogeneous chemistry played in the production of NO_3^- in the atmosphere (Michalski et al., 2003). Here, the authors attributed the seasonal variation of the isotopic composition of bulk aerosol nitrate to shifts in the relative importance of homogeneous and heterogeneous chemistry in a polluted marine boundary layer. Specifically, the predominant homogeneous oxidation pathways used by the authors were:

$$NO_2 + OH + M \rightarrow HNO_3(g) + M \quad \text{(R1)}$$

$$NO_2 + O_3 \rightarrow NO_3 + O_2 \quad \text{(R2)}$$

$$NO_3 + HC, DMS \rightarrow HNO_3(g) + \text{products} \quad \text{(R3)}$$

ACPD
9, 13355–13406, 2009

Gaseous nitric acid may then be taken up by aerosols to become atmospheric nitrate. The heterogeneous production of aerosol nitrate specified by Michalski et al. (2003) was given as:

$$NO_2 + NO_3 \leftrightarrow N_2O_5 + H_2O(surf.) \rightarrow HNO_3(aq) \quad \text{(R4)}$$

While only Reaction (R2) appears to result in the transfer of an excess of ^{17}O from O_3 , a detailed examination of the NO_x photochemical cycle reveals that the role of the shared precursor, NO_2, is important as well.

The oxygen isotopic composition of NO_2 and O_3 are expected to be linked via the following photochemical reactions:

$$NO + O_3 \rightarrow NO_2 + O_2 \quad \text{(R5)}$$

$$NO_2 + h\nu \rightarrow NO + O(^3P) \quad \text{(R6)}$$

$$O(^3P) + O_2 + M \rightarrow O_3 \quad \text{(R7)}$$

An additional source of oxygen atoms for NO_2 are reactions with HO_2 or peroxy radicals (RO_x):

$$NO + HO_2(RO_x) \rightarrow NO_2 + OH(RO) \quad \text{(R8)}$$

During daytime conditions, Reactions (R5) through (R8) occur rapidly and the oxygen isotopic composition of NO_2 is expected to converge and be set by the relative contributions from reactions R5 and R8 and their respective $\Delta^{17}O$ values. In general, it is assumed that $\Delta^{17}O(HO_2) \simeq 0$ (Michalski et al., 2003), although we will examine the validity of this assumption later in this paper. While measurements of the isotopic composition of O_3 are not typically available, field measurements of its bulk isotopic composition have yielded values from as low as 21‰ to as high as 32‰ (Johnston and Thiemens, 1997). These values are lower than those assumed by previous modeling studies which assumed bulk ozone $\Delta^{17}O$ enrichments of about 35‰ (Lyons, 2001; Michalski et al., 2003; Zahn et al., 2006; Morin et al., 2007b).

Recently it was shown that Reaction (R5) results in the preferential transfer of a terminal atom in O_3 with a frequency >92±5% (Savarino et al., 2008) and the magnitude of the enrichment found in the central and terminal atoms was determined experimentally by Bhattacharya et al. (2008). Here the authors found that the isotopic composition of O_3 made in the laboratory has a $\Delta^{17}O \simeq 25‰$ and the terminal atoms relatively enriched, having a $\Delta^{17}O \simeq 35‰$. These finding are important since O_3 photolysis is a major source of OH in the atmosphere as shown by:

$$O_3 + h\nu \rightarrow O_2 + O(^1D) \quad \text{(R9)}$$

$$O(^1D) + H_2O \rightarrow 2OH \quad \text{(R10)}$$

$O(^1D)$ produced from this reaction is expected to have a large $\Delta^{17}O$ and may also transfer its isotopic anomaly to other oxygen species in the atmosphere as shown by Lyons (2001).

Isotopic exchange reactions such as:

$$H_2O + QH \leftrightharpoons H_2Q + OH \quad \text{(R11)}$$

will also affect the isotopic composition of oxygen bearing compounds in the atmosphere and the exchange Reaction (R11) between H_2O ($\Delta^{17}O$=0‰) and OH and may completely erase the excess ^{17}O of OH acquired from $O(^1D)$. Because of how rapidly this exchange reaction proceeds under tropospheric conditions (Greenblatt and Howard, 1989), it is generally assumed that $\Delta^{17}O(OH)=0$. The validity of this often used assumption will be directly tested in this paper.

4.1 The conservative nature of mass-independent isotopic signatures

Isotopic fractionation associated with most physical processes, such as the evaporation of water from a reservoir, may systematically favor the retention or depletion of "lighter" isotopomers (e.g. $H_2^{16}O$ vs. $H_2^{18}O$) due to kinetic or equilibrium isotope effects. These processes will in general change the ^{16}O, ^{17}O, and ^{18}O content of atmospheric

compounds, but in a *mass-dependent* manner and as a result the $\Delta^{17}O$ composition of a reservoir of molecules is conserved unless there is mixing of additional molecules with a different $\Delta^{17}O$. A thorough review of the nature of mass-dependent and mass-independent fractionations for oxygen and sulfur was recently published (Thiemens, 2006).

5 Photochemical modeling the $\Delta^{17}O$ of oxygen bearing species in a Polluted Urban Boundary (PUB) layer

The Polluted Urban Boundary Layer (PUB) model is a photochemical box model (written in Matlab) with three main components:

1. A chemical model for calculating the time evolution of over 41 chemical species using over 138 chemical and photochemical reactions as detailed in (Yvon et al., 1996).
2. An aerosol surface area distribution submodel for heterogeneous loss and chemistry (e.g. $N_2O_5+H_2O(surf) \rightarrow HNO_3(aq)$).
3. An isotope ratio ($\Delta^{17}O$) submodel for tracking the time evolution of the ^{17}O anomaly in oxygen bearing species, not including water vapor, ozone, and molecular oxygen in the atmosphere.

Of particular importance to the results presented here is the inclusion of a sea-salt aerosol distribution to calculate the effects of heterogeneous production of HNO_3 on these particles given by Reaction (R4).

5.1 Chemical species and time dependent chemistry

The concentration of chemical species in PUB are tracked and integrated using 4th order Runge-Kutta integration (Press et al., 2002). Actinic fluxes, photolysis rates

and quantum efficiencies are calculated for NO_2, NO_3, H_2O_2, HNO_2, HNO_3, HO_2NO_2, N_2O_5, CH_3OOH, HCO, CH_3C as described in Yvon et al. (1996) and Yvon and Saltzman (1993).

Input parameters include temperature (T), relative humidity (RH), NO_x flux, O_3 concentration, boundary layer height (BLH), total ozone column density, and cloud albedo. These factors are known to affect the oxidative conditions of the marine boundary layer and can be changed or held constant in the model. Combined with the oxygen isotopes submodel (Sect. 5.2) they can used to probe the sensitivity of $\Delta^{17}O$ in atmospheric species to environmental variables. The results of these sensitivity tests are presented in Sect. 6.

5.2 Oxygen isotopes submodel

The PUB model calculates the time dependent $\Delta^{17}O$ values of a chemical species using a weighted average approach that provides isotopic mass-balance. This procedure calculates the $\Delta^{17}O$ of a chemical species X as follows:

$$\Delta^{17}O\,(X(i+1))\,[X(i+1)] = \Delta^{17}O(X(i))\,[X(i)] + \sum_{\text{sources,j}} d[X_j(i)]\Delta^{17}O(d\,[X_j(i)]) \quad (2)$$

where [X(i)] represents the concentration of species X, $\Delta^{17}O\,(X)$ is the isotopic anomaly associated with species X, $d\,[X_j]$ is an infinitesimal change in that concentration from a chemical/photochemical reaction j, and $\Delta^{17}O(d\,[X_j(i)])$ is the anomaly transferred by that source. We assume that all sink reactions do not affect the $\Delta^{17}O$ of species, which is equivalent to saying that they are mass dependent.

The amount of $\Delta^{17}O$ transferred by source reaction j will depend on the number of oxygen atoms in the product X_j derived from the reactants and the $\Delta^{17}O$ associated with these. For example, the $\Delta^{17}O$ of the homogeneous Reaction (R1) is given by:

$$\Delta^{17}O(d[HNO_3(g)]) = \frac{2}{3}\Delta^{17}O\,(NO_2) + \frac{1}{3}\Delta^{17}O\,(OH) \quad (3)$$

ACPD
9, 13355–13406, 2009

The origin of any excess ^{17}O found in atmospheric species is assumed to originate from O_3 and is propagated to other atmospheric species and warrants further discussion.

5.2.1 $\Delta^{17}O$ of O_3, $O(^1D)$, NO_2, and OH

Following the suggestion by Savarino et al. (2008) and in agreement with previous isotopic measurements of the $\Delta^{17}O$ of tropospheric O_3 (Krankowsky et al., 1995; Johnston and Thiemens, 1997), the $\Delta^{17}O$ of bulk ozone was assumed to be constant and fixed at 25‰. The central and terminal position anomalies were detemined using a linear fit to the inferred relationship between the bulk and terminal as well as central positions of the $\Delta^{17}O$ of O_3 reported in (Bhattacharya et al., 2008):

$$\Delta^{17}O(O_3(\text{terminal})) = (0.97 \pm 0.1\,(2\sigma))\Delta^{17}O(O_3(\text{bulk})) + 13\ ‰ \quad (4)$$

$$\Delta^{17}O(O_3(\text{central})) = (0.91 \pm Y\,(2\sigma))\Delta^{17}O(O_3(\text{bulk})) - 25\ ‰ \quad (5)$$

These details on the distribution of ^{17}O in O_3 are important since in the UV photolysis of O_3,

$$O_3 + h\nu \rightarrow O_2 + O(^1D) \quad (R12)$$

it is expected that on average $O(^1D)$ originates from the terminal position at least 91% of the time, resulting in an elevated heavy isotopic enrichment $O(^1D)$. For our calculations, we assumed that:

$$\Delta^{17}O\left(O(^1D)\right) = 0.91 \times \Delta^{17}O\,(O_3(\text{terminal})) +$$

$$0.09 \times \Delta^{17}O\,(O_3(\text{central})) \quad (6)$$

$$= 34.76‰ \quad (7)$$

With the exception of water vapor ($\Delta^{17}O$=0‰), molecular oxyygen ($\Delta^{17}O$= 0‰), and ozone ($\Delta^{17}O$(bulk)=25‰) which we consider to be infinite reservoirs here, all other starting values of $\Delta^{17}O$ were assumed to equal zero initially, but were allowed to acquire an ^{17}O excess via their precursors and isotopic exchange as described in Eq. (2) and Reaction (R11). We neglect the effect of chemical reactions such as CO+OH→CO_2+H and H+O_2+M which are known to produce CO_2 and HO_2 with $\Delta^{17}O \neq 0$ (Huff and Thiemens, 1998; Rockmann et al., 1998; Savarino and Thiemens, 1999b). Of particular importance to species like $\Delta^{17}O$(OH), whose precursor $O(^1D)$ has a large ^{17}O anomaly, the exchange Reaction (R11) is treated numerically as a chemical reaction that takes away OH with $\Delta^{17}O \neq O$ followed by a production of the same amount of OH with a $\Delta^{17}O$=0. A list of exchange reactions considered in our numerical implementation of isotopic exchange are given below Reactions (R13–R15) and their respective rate constants are summarized in Table 1.

$$QH + H_2O \rightleftharpoons OH + H_2Q \quad (R13)$$

$$NQ + OH \rightleftharpoons NO + QH \quad (R14)$$

$$HOQ + OH \rightleftharpoons HOO + QH \quad (R15)$$

5.3 Aerosol surface area submodel

To examine the role that differential uptake of precursors of nitrate may have on the $\Delta^{17}O$ of aerosol nitrate as a function of size, the PUB model aerosol submodel can be used to specify an arbitrary number of aerosol size bins, each with chemical compound specific uptake coefficients. For the purpose of examining the maximum contrast between $\Delta^{17}O$ of nitrate as a function of aerosol size, we specified two surface area size bins, a fine (F, Diameter≤1.5 μm) and a coarse (C, Diameter>1.5 μm). For each of

these size bins, deposition losses are calculated by specifying a deposition timescale, τ_d. For all of the data presented here, we assumed that the fine and coarse size bins had τ_d(F)=6 h and τ_d(C)=10 days to roughly correspond to the deposition timescales expected for fine sulfate dominated particles and coarse-sized sea-salt spray. The concentration and isotopic composition of nitrate in each of these size bins are treated exactly like the gas-phase species in the PUB model and we assume that the deposition process does not fractionate our aerosol nitrate in a mass-independent manner.

5.3.1 Size-dependent $\Delta^{17}O(NO_3^-)$: the role of aerosol surfaces area types

Previous triple-oxygen isotope measurements of NO_3^- in size-segregated aerosols in a pristine MBL by Patris et al. (2007) found that nitrate found in coarse particles (NO_3^-(C)) had a consistently higher $\Delta^{17}O$ compared to nitrate found in fine particles (NO_3^-(F)). These results were interpreted as direct evidence of N_2O_5 uptake onto sea-salt particles. In their work, Michalski et al. (2003) used a single aerosol surface area concentration ($\mu m^2\,cm^{-3}$) to track their aerosol nitrate and thus provide no specific insight into the relative importance of this process.

For the sensitivity studies described in the next section, the available aerosol surface area was represented simply as a combination of an urban (<1.5 μm) and a sea-salt aerosol distribution (>1.5 μm) and the uptake of gas-phase species X is calculated using the first-order reaction rate for uptake:

$$\frac{d[X]}{dt} = \frac{\gamma}{4} c[X] A \qquad \text{(R16)}$$

where the molecular speed $c=\sqrt{\frac{8k_bT}{\pi m_x}}$, m_x is the mass of species X, γ is the sticking probability of species X of the surface of aerosols with a surface area concentration A, and k_b is Boltzmann's constant. For the calculations we present here, we assumed that γ=0.1 for HNO_3 for both coarse and fine aerosol surfaces. Aqueous sea-salt particles were set to dominate the coarse aerosol surface area and the uptake of N_2O_5

($\gamma(N_2O_5)$=0.05) and HNO_3 produced aerosol nitrate in the coarse size-bin while only N_2O_5 was assumed to be taken up in the coarse (aqueous) aerosol size bin. This size-dependent aqueous surface may potentially produce size dependent $\Delta^{17}O$ values in aerosol nitrate (Seinfeld and Pandis, 2006).

The residence time of aerosols, while not directly a factor in determining their isotopic composition, provides inertia for rapid changes in the average isotopic composition of aerosol nitrate and this effect is also accounted for in the aerosol sub-model as a sink reaction for aerosol nitrate in the fine (F) and coarse (C) size bins.

6 Sensitivity study of $\Delta^{17}O$ of atmospheric species

Conventionally, sample size requirements for the triple-oxygen isotopic analysis of aerosol nitrate have demanded that aerosol sampling be done over time periods ranging from 12–36 h for typical aerosol nitrate concentrations. During this time, environmental parameters such as temperature, relative humidity, NO_x flux, etc. may vary. Advances in analytical capabilities have reduced the sample size and the potential for high time-resolution measurements of the triple-isotopic composition of atmospheric species exists (Kaiser et al., 2007). At either range of time-scales, the oxidizing conditions and hence the $\Delta^{17}O$ of atmospheric species may have substantially diurnal variability. Finally, regional and long-range transport of species may also influence the isotopic composition of NO_y and HO_x species, further motivating the study of $\Delta^{17}O$ as a function of geographic and anthropogenic factors. To explore these issues, we specified baseline conditions and changed variables individually to probe the numerical sensitivity of $\Delta^{17}O$ of major oxygen bearing species to these factors. The list of environmental variables and their baseline values are summarized in Table 2.

The sensitivity of the following NO_y species: NO, NO_2, NO_3, HNO_3, N_2O_5, and fine (NO_3^-(F)) and coarse aerosol nitrate (NO_3^-(C)) are reported in the next section. The range of observed $\Delta^{17}O$ of other oxygen bearing trace species (e.g. PAN, HNO_2,

HNO_2) calculated by the PUB model are summarized in Table 3.

The bulk of our discussion will focus on major species whose $\Delta^{17}O$ have previously been measured or inferred and used in calculations of important precursors to measured species. These precursors include: OH, H_2O_2, HO_2, NO,NO_2, HNO_3,N_2O_5, and aerosol NO_3^-. To control for model dependence on initial conditions, the model was first run for 150 h to ensure numerical convergence. While the daily average $\Delta^{17}O$ are typically well converged at this timescale, most species display large diurnal variations in both their concentration and isotopic composition, which are expected to be due to the photochemical production of OH and isotope exchange with water vapor during daylight conditions. To illustrate this dynamic, we plot the concentration of [OH] and $\Delta^{17}O$ of HNO_3 vs. time for a baseline run where $[O_3]$=1 ppmv in Fig. 1.

We provide plots of $\Delta^{17}O$ of NO_y as well as OH and $HO_2$for a select number of the variables tested in our study. For all other variables, we summarize their influence on $\Delta^{17}O$ of oxygen bearing species in Sect. 6.7. When reporting the results of our sensitivity study in plots, we will report both the time-average $\Delta^{17}O$ values of species for the last 24 h of model run time (out of 150) as well as the diurnal variation (min,max) of these using diagonal or vertical bars.

6.1 Sensitivity to relative humidity

6.1.1 NO_y

Depending of geographic location and associated meteorology, the diurnal range in relative humidity (RH) can be mild or extreme. We plot the sensitivity of $\Delta^{17}O$ vs. RH of key NO_y species in Fig. 2. Examination of this plot shows that $\Delta^{17}O$ is relatively sensitive to humidity, especially at low RH values, but decreases at higher RH. The inverse correlation between $\Delta^{17}O$ and RH is not surprising given that the abundance of water vapor in the atmosphere directly influences both the rate of isotopic exchange between H_2O vapor and OH as well as the abundance of OH. This interplay between

[OH] and oxygen bearing species was seen in all of our simulations, and contribute to the significant variability of $\Delta^{17}O(HNO_3)$. These results suggest that actinic flux variability during sampling with high time resolutions ($\Delta t \sim 1-6$ h), could be sensitive this effect, especially near strong NO_x sources. Finally, we note that the differences in $\Delta^{17}O$ of nitrate *produced* in fine and coarse particles did not differ by more than 0.3‰ for all of the environmental conditions that we probed in this study.

6.1.2 HO_x and H_2O_2

In exploring the effects of RH on $\Delta^{17}O$ values of HO_x and H_2O_2 shown in Fig. 3, we make note of several things:

- The time-averaged $\Delta^{17}O(HO_2)$ is significantly greater than 0‰ and has significant diurnal variability
- The time-averaged $\Delta^{17}O(OH)$ becomes significant (25‰) as RH→0
- The time-averaged $\Delta^{17}O(H_2O_2)$ is a function of RH, converging at about 2‰ RH≥30 %

The origin of the significant $\Delta^{17}O$ values of HO_2 seen here will be discussed later in this paper (See Sect. 7.1).

6.2 Sensitivity to $[O_3]$

6.2.1 NO_y

Plots of $\Delta^{17}O$ vs. $[O_3]$ for NO_y and aerosol NO_3^- are shown in Fig. 4. The lower end of O_3 concentrations was chosen to reflect the oxidative conditions present in a relatively pristine environment such as a rain forest or a remote marine boundary layer, while the higher end were chosen to be representative of those fond in a polluted urban

area (CITE HERE). In examining Fig. 4, it is clear that $\Delta^{17}O$ of aerosol nitrate and its precursors are sensitive non-linear functions of O_3 concentrations.

6.2.2 HO_x and H_2O_2

Interestingly, the time-averaged $\Delta^{17}O(HO_2)$ does not appear to be sensitive to $[O_3]$, while the $\Delta^{17}O(H_2O_2)$ appears to be sensitive to $[O_3]$ (see Fig. 5).

6.3 Sensitivity to NO_x Flux

6.3.1 NO_y

The rates of NO_x flux into the atmosphere can vary by orders of magnitude ($1–10^4$ μmoles m^{-2} dy^{-1}) and these are dominated by anthropogenic activities (GEIA-ACCENT Database, 2005). To explore the sensitivity of $\Delta^{17}O$ of NO_y and aerosol nitrate to this variable, we varied NO_x flux from 0–200 μmoles m^{-2} dy^{-1}. These results are shown in Fig. 6. It should be noted that in all of our simulations, O_3 concentrations were fixed to explore the role that increases in NO_x flux have of $\Delta^{17}O$ for the species we studies. We acknowledge that holding the concentration of O_3 constant while increasing NO_x fluxes may be unphysical, but this treatment avoids the complexities of generating ozone via organic precursors while still allowing us to probe the numerical consequences of increasing NO_x flux. It is interesting to note that both O_3 and NO_x flux are significant influences in the $\Delta^{17}O$ of NO_y species and that this contrast appears to saturate in environments with strong NO_x sources.

6.3.2 HO_x and H_2O_2

We note that the $\Delta^{17}O$ of H_2O_2 in high NO_x flux environments (Fig. 7) goes to zero, suggesting a source of variation for the $\Delta^{17}O$ of H_2O_2 measurements in the environment. The $\Delta^{17}O$ values of HO_2 and OH appear to increase systematically as a function

of NO_x flux. This effect would explain some, but not all, of the associated increases in $\Delta^{17}O$. In any case, these results suggest that assessments of the $\Delta^{17}O$ calculations of the $\Delta^{17}O$ of atmospheric species in plumes will likely require explicit numerical isotopic determinations such as these.

6.4 Sensitivity to CH_4

6.4.1 NO_y, HO_x and H_2O_2

Global methane levels, as deduced from ice core data, show that methane concentrations have ranged from about 0.350–0.700 ppmv over the last 420 000 (Petit et al., 1999). Strong regional sources of methane are known to exist (Owens, 1991). With this variability in mind, we plot the $\Delta^{17}O$ of NO_y and aerosol NO_3^- a function $[CH_4]$ in Fig. 8. These results indicate that local oxidizing conditions perturbed by significant amounts of methane, such as agricultural centers, may have a significant effect on $\Delta^{17}O$ of NO_y. In contrast, increased methane concentrations appear to have a mild effect on $\Delta^{17}O$ of HO_x(Fig. 9).

6.5 Sensitivity to latitude

6.5.1 NO_y

The sensitivity of $\Delta^{17}O$ of NO_y and aerosol NO_3^- to the latitude of their production are shown in Fig. 10. Changes in latitude are equivalent to changes in zenith angle and illustrate the potential sensitivity of NO_y species to the geographic location where these species are oxidized. These results also suggest that NO_y transported from sources at different latitudes may be distinguished from locally produced NO_y species if isotopic exchange or mixing between these is precluded. The asymmetrical dependence seen in Figs. 10 and 11 is due to the baseline Julian Day chosen for this run (Julian Day=5), and indicates that this sensitivity is enhanced during during the winter season for both

the Northern and Southern Hemispheres. We note that if the simulations had been run at either Spring or Fall Equinox, we would expect a symmetrical dependence on latitude.

6.5.2 HO_x and H_2O_2

It is interesting to note that the $\Delta^{17}O$ of HO_2 is also strongly dependent on latitude, while H_2O_2 is relatively insensitive except at the highest latitudes, where it decreases to zero in our simulations.

6.6 Sensitivity to cloud albedo

6.6.1 NO_y

We explored the sensitivity of $\Delta^{17}O$ vs. cloud albedo of NO_y and aerosol NO_3^- by varying the cloud albedo. These results are shown in Fig. 13. Over the range of 0-1 for cloud albedo, we find that values below 0.5 have a negligible effect on the $\Delta^{17}O$ of NO_y with the sensitivity being increasingly non-linear at cloud albedo values above 0.5. These results suggest that cloud albedo is a significant variable in determining the $\Delta^{17}O$ of NO_y an aerosol nitrate.

6.6.2 HO_x and H_2O_2

It is interesting to note that while the $\Delta^{17}O$ of HO_2 increases as cloud albedo $\rightarrow$1, the $\Delta^{17}O$ of H_2O_2 decreases to zero.

6.7 Other sensitivities

We summarize results of other sensitivity tests in Table 4. Some variables such as Temperature and cloud base height appear to have very little effect on the $\Delta^{17}O$ of

aerosol NO_3^- while ozone column density, boundary layer height, and Julian Day do have a measurable effect.

While we have not treated the formation of aerosol sulfate in our modeling study, we note that increases in the flux of atmospheric S in the forms of Dimethylsulfide (DMS) and H_2S both led to increases in the $\Delta^{17}O$ of NO_y and aerosol NO_3^-. An examination of model output [OH] concentrations as a function of these two variables suggest that the additional inputs of S into the atmosphere, some of which become SO_2, in turn lead to systematic decreases in the concentration of [OH] and a decrease in the fraction of all aerosol nitrate produced by Reaction (R1). Further studies using a coupled N and S isotopic model should be carried out to further investigate the possibility of this being a significant factor in $\Delta^{17}O$ studies.

7 Comparison with analytic determinations of $\Delta^{17}O$ of HO_2 and NO_2

7.1 $\Delta^{17}O$ of HO_2

Our explicit calculations of $\Delta^{17}O(HO_2)$ suggest that the time averaged $\Delta^{17}O$ of HO_2 has a large diurnal variation and is significantly higher ($\Delta^{17}O \sim 10$–$30‰$) than zero for a wide range of atmospheric conditions. The concentration averaged values, on the other hand, are closer to zero, though these are still significantly higher than zero. The source of this surprising result merits further discussion as the sources of HO_2 considered in our model are:

$$H + O_2 + M \rightarrow HO_2 \; [\Delta^{17}O \simeq 0‰] \quad \text{(R17)}$$

$$OH + O_3 \rightarrow HO_2 + O_2 \; [\Delta^{17}O \gg 0‰] \quad \text{(R18)}$$

$$OH + H_2O_2 \rightarrow HO_2 + H_2O \; [\Delta^{17}O \simeq \frac{1}{2}\Delta^{17}O(H_2O_2)] \quad \text{(R19)}$$

$$HO_2NO_2 \rightarrow HO_2 + NO_2 \; [\Delta^{17}O = \Delta^{17}O(HO_2NO_2)] \quad \text{(R20)}$$

Estimates of the relative importance of these sources for representative atmospheric conditions experienced in the simulations run are summarized in Table 5. Based on the concentrations of ozone, H, and OH, it is clear that Reaction (R20) is a significant production pathway for HO_2 in the atmosphere, especially at night when photochemical production channels of OH and H diminish and the photolysis of HO_2 ceases. The major question regarding the production of HO_2 via Reaction (R20) is what should the $\Delta^{17}O$ of the HO_2 produced be, given that the major source of HO_2NO_2 is:

$$HO_2 + NO_2 \rightarrow HO_2NO_2 \quad \text{(R21)}$$

In our numerical scheme (Sect. 5.2), the $\Delta^{17}O$ of newly produced HO_2NO_2 by Reaction (R21) is given by:

$$\Delta^{17}O(d[HO_2NO_2]) = \frac{1}{2}\left[\Delta^{17}O(HO_2) + \Delta^{17}O(NO_2)\right] \quad \text{(R22)}$$

This scheme is responsible for the higher than expected $\Delta^{17}O$ values for HO_2 even in the absence of the mass-independent chemistry that has been previously reported for HO_x formation (Savarino and Thiemens, 1999b).

So why has this pathway been previously overlooked? In part, assuming that $\Delta^{17}O(HO_2)$~2‰ seems reasonable given that $HO_2 + HO_2 \rightarrow H_2O_2$ is a major production pathway of H_2O_2 and the finding by Savarino and Thiemens (1999a) that $\Delta^{17}O(H_2O_2)$~2‰.

7.2 $\Delta^{17}O$ of NO_2

Here we compare the $\Delta^{17}O$ produced using our explicit calculations and those obtained using the approximations and chemical partitioning approach used by others (Michalski et al., 2003; Kunasek et al., 2008). To control for differences in the details of producing aerosol nitrate production, we focus on the $\Delta^{17}O$ of NO_2. In general previous work has

approximated the $\Delta^{17}O$ of $NO_2$by using the outputs of chemical models, calculating a partition ratio *A*. Following Kunasek et al. (2008), this partition variable is:

$$A = \frac{\left(\frac{d[NO_2]}{dt}\right) O_3 path}{\left(\frac{d[NO_2]}{dt}\right)_{total}} \quad (8)$$

$$= \frac{k_1[O_3][NO]}{k_1[O_3][NO] + k_2[HO_2][NO] + k_3[RO_2][NO]} \quad (9)$$

The $\Delta^{17}O$ of NO_2 is then calculated as:

$$\Delta^{17}O(NO_2) = A \times \Delta^{17}O(O_3 - \text{trans.}) \quad (10)$$

Here $\Delta^{17}O(O_3\text{-trans.})$ is the average value transferred to NO_2 from ozone. To directly compare to the results of Kunasek et al. (2008), $\Delta^{17}O(O_3 - \text{trans.})$ will be assumed to be 35 ‰ . The rate constants used are:

$$k_1 = 3 \times 10^{-12} \exp(-1500/T) \quad (11)$$

$$k_2 = 3.5 \times 10^{-12} \exp(250/T) \quad (12)$$

As prescribed in Kunasek et al. (2008), we also assume that $k_3[RO_2][NO] = \frac{1}{2}k_2[HO_2][NO]$.

So how do the analytic and explicit calculations compare? Using concentrations provided by the PUB model chemical submodel, we calculate the expected $\Delta^{17}O(NO_2\text{-anal.})$ and compared these to the results provided by PUB's isotopic sub-model(See Sect. refsec:isotopesubmodel). The difference between our presumably more exact treatment of $\Delta^{17}O$ anomaly transfer and the analytic approximations used is defined as:

$$\epsilon(NO_2) = \Delta^{17}O(\text{numeric}) - \Delta^{17}O(\text{anal.}) \quad (13)$$

ACPD
9, 13355–13406, 2009

In general, we found significant differences in the $\Delta^{17}O$ calculated by our numeric approach compared to the partition ratios method used by others. Not all of these differences can be attributed solely to the effect of having a non-zero $\Delta^{17}O$ for HO_2 since the calculated differences ($\epsilon(NO_2)$) ranged from about −7 ‰ to +3‰. The origins of these differences are subtle, likely reflecting systematic changes in the $\Delta^{17}O$ values and concentrations of HO_2, H, and OH. To illustrate the non-linear nature of these differences, we plot $\epsilon(NO_2)$ as a function of relative humidity and total ozone column density in Figs. 14 and 15.

8 Conclusions

We have developed and presented a simple isotopic photochemical box model for explicitly calculating the $\Delta^{17}O$ of major oxygen bearing species in the atmosphere. Using this photochemical model, we have probed the sensitivity of the triple-oxygen isotopic compositions ($\Delta^{17}O$) of important oxygen bearing species to atmospheric conditions that may vary at the local, regional, and global scales.

As a result of these sensitivity tests, we have shown that the $\Delta^{17}O$ of aerosol NO_3^- is expected to vary as functions of environmental factors such as relative humidity, cloud albedo, anthropogenic influences and urban setting and that these shifts and their diurnal variation are significant in the precursors of aerosol nitrate. Some of these variables may or may not vary independently of each other (e.g. relative humidity and cloud cover), but by varying each of these factors individually, we have isolated their potential contributions to atmospheric sample variability.

The results presented on the relationship between NO_x flux and $\Delta^{17}O$ in nitrate are consistent with the observations of Alexander et al. (2004), which found a shift in the $\Delta^{17}O$ of Greenland ice-core NO_3^- ($\simeq$2‰) that was directly tied to an increase in pre-industrial biomass burning in North America.

The sensitivity of $\Delta^{17}O$ of NO_y species to ozone and total ozone column density suggest a potential source of variability in Antarctic samples. Photochemical models

of $\Delta^{17}O$ of NO_y should consider the contribution that both of these factors make. The results of $\Delta^{17}O$ of NO_3^- versus total ozone column density suggests that these may be correlated, not anti-correlated as suggested by McCabe et al. (2007).

In all of our tests, we found that the $\Delta^{17}O$ of nitrate in fine and coarse aerosols rarely deviated from each other by more than 0.3‰. These results strongly suggest that size-dependent deviations exceeding this amount may indicate the mixing of distinct sources of NO_y with distinct oxidative conditions.

We have found, as result of our explicit numerical calculations, that contrary to assumptions regarding the $\Delta^{17}O$ of OH, H_2O_2 and HO_2 made by previous authors (Michalski et al., 2003; Savarino and Thiemens, 1999a; Alexander et al., 2004; Kunasek et al., 2008; Alexander et al., 2009), our explicit tracking of $\Delta^{17}O$ for these species and their precursors shows that their $\Delta^{17}O$ is expected to vary as a function of NO_x-O_3 environment. In addition, we have shown that HO_2 can have $\Delta^{17}O$ values that are significantly greater than zero.

As a result of our explicit calculations of the $\Delta^{17}O(NO_2)$, we have shown that analytical approximations used by previous models of NO_x chemistry may significantly under or overestimate the $\Delta^{17}O$ of NO_y species as well as HO_2 and our overall results suggest that other factors such as methane and S sources may need to be considered when interpreting $\Delta^{17}O$ measurements of atmospheric species.

Given our explicit calculations, we provide the first calculations of atmospheric H_2O_2. These calculations show that the $\Delta^{17}O$ of H_2O_2 obtains some if not all of its anomaly through O_3. In this context, it should be noted that previous modeling work by Zahn et al. (2006) predicted non-zero values for HO_2 in the middle atmosphere while Lyons (2001), by considering the isotopic exchange reaction between HO_2 and O_2, found that this completely erased the ^{17}O anomaly. More laboratory measurements of poorly constrained isotope exchange rates, as suggested by Zahn et al. (2006), are needed to provide a definitive answer to this question, but our results suggest that the entire anomaly found in atmospheric H_2O_2 does not require chemical mass-independent ori-

gins as suggested by Savarino and Thiemens (1999b).

Finally, our model results suggest that explicit calculations of the $\Delta^{17}O$ of atmospheric oxygen bearing species, using the general algorithm presented (Eq. 2) here should be implemented in the global chemistry models of $\Delta^{17}O$ (e.g. Alexander et al., 2005) and point to the importance of local and regional conditions in determining the isotopic composition of aerosol nitrate, NO_y and HO_xspecies in the atmosphere.

Appendix A

Notation

The isotopic ratios of a sample (SA) can be quantified with respect to an isotopic standard (ST). For oxygen, the Standard Mean Ocean Water (SMOW) standard is used and the isotope ratios of samples are quantified as:

$$\delta^{x}O(‰) = \left(\frac{{}^{x}R_{SA}}{{}^{x}R_{ST}} - 1\right) \times 1000 \quad \text{(A1)}$$

where ${}^{x}R_{SA,ST} = \frac{[{}^{x}O_{SA,ST}]}{[{}^{16}O_{SA,ST}]}$ and $x = 17$ or 18.

Acknowledgements. We would like to thank S. Yvon for her generous access to the PBMAC Fortran code and documentation. Lauren Brothers, Subrata Chakraborty, Terri Jackson, Justin McCabe, and Robina Shaheen are acknowledged for helpful discussions. G. D. acknowledges the Camille and Henry Dreyfus Postdoctoral Program in Environmental Chemistry as well as the University of California's Presidents Fellowship Program for their financial support.

References

Alexander, B., Savarino, J., Kreutz, K. J., and Thiemens, M. H.: Impact of preindustrial biomass-burning emissions on the oxidation pathways of tropospheric sulfur and nitrogen, J. Geophys. Res. Atmos., 109, 8303, doi:10.1029/2003JD004218, 2004. 13359, 13379, 13380

Alexander, B., Park, R. J., Jacob, D. J., Li, Q. B., Yantosca, R. M., Savarino, J., Lee, C. C. W., and Thiemens, M. H.: Sulfate formation in sea-salt aerosols: Constraints from oxygen isotopes, J. Geophys. Res. Atmos., 110, 10307, doi:10.1029/2004JD005659, 2005. 13381

Alexander, B., Hastings, M. G., Allman, D. J., Dachs, J., Thornton, J. A., and Kunasek, S. A.: Quantifying atmospheric nitrate formation pathways based on a global model of the oxygen isotopic composition (?17O) of atmospheric nitrate, Atmos. Chem. Phys. Discuss., 9, 11185–11220, 2009, http://www.atmos-chem-phys-discuss.net/9/11185/2009/. 13360, 13380

Alexander, B., Hastings, M. G., Allman, D. J., Dachs, J., Thornton, J. A., and Kunasek, S. A.: Quantifying atmospheric nitrate formation pathways based on a global model of the oxygen isotopic composition ($\Delta^{17}O$) of atmospheric nitrate, Atmos. Chem. Phys. Discuss., 9, 11185–11220, 2009, http://www.atmos-chem-phys-discuss.net/9/11185/2009/. 13357

Bao, H. and Gu, B.: Natural Perchlorate Has a Unique Oxygen Isotope Signature, Environ. Sci. Technol., 38, 5073–5077, doi:10.1021/es049516z, 2004. 13357

Bao, H., Campbell, D. A., Bockheim, J. G., and Thiemens, M. H.: Origins of sulphate in Antarctic dry-valley soils as deduced from anomalous ^{17}O compositions, Nature, 407, 499–502, 2000a. 13357

Bao, H., Thiemens, M. H., Farquhar, J., Campbell, D. A., Lee, C. C.-W., Heine, K., and Loope, D. B.: Anomalous ^{17}O compositions in massive sulphate deposits on the Earth, Nature, 406, 176–178, 2000b. 13357

Bao, H., Lyons, J. R., and Zhou, C.: Triple oxygen isotope evidence for elevated CO_2 levels after a Neoproterozoic glaciation, Nature, 453, 504–506, 2008. 13357

Bhattacharya, S. K., Pandey, A., and Savarino, J.: Determination of intramolecular isotope distribution of ozone by oxidation reaction with silver metal, J. Geophys. Res. Atmos., 113, 3303, doi:10.1029/2006JD008309, 2008. 13360, 13364, 13367

Brothers, L. A., Dominguez, G., Fabian, P., and Thiemens, M. H.: Using multi-isotope tracer methods to understand the sources of nitrate in aerosols, fog and river water in Podocarpus

National Forest, Ecuador, Eos Trans. AGU, 89, Abstract A11C-0136, 2008. 13360
Cliff, S. S. and Thiemens, M. H.: The 18O/16O and 17O/16O Ratios in Atmospheric Nitrous Oxide: A Mass-Independent Anomaly, Science, 278, 1774–1776, doi:10.1126/science.278.5344.1774, 1997. 13357
Dominguez, G., Jackson, T., Brothers, L., Barnett, B., Nguyen, B., and Thiemens, M. H.: Discovery and measurement of an isotopically distinct source of sulfate in Earth's atmosphere, Proceedings of the National Academy of Sciences, 105, 12769–12773, doi:10.1073/pnas.0805255105, 2008. 13357, 13360
Dransfeld, P. and Wagner, H. G.: Comparative study of the reactions of ^{16}OH and ^{18}OH with H^{16}O$_2$, Naturforsch, 41a, 1283–1288, 1987. 13387
Dubey, M. K., Mohrschladt, R., Donahue, N. M., and Anderson, J. G.: Isotope Specific Kinetics of Hydroxyl Radical (OH) with Water (H2O):Testing Models of Reactivity and Atmospheric Fractionation, The Journal of Physical Chemistry A, 101, 1494–1500, doi:10.1021/jp962332p, 1997. 13387
GEIA-ACCENT Database: an international cooperative activity of AIMES/IGBP,, sponsored by the ACCENT EU Network of Excellence, http://www.accent-network.org, 2005. 13373
Greenblatt, G. D. and Howard, C. J.: Oxygen atom exchange in the interaction of hydroxyl-(^{18}OH) with several small molecules, The Journal of Physical Chemistry, 93, 1035–1042, doi:10.1021/j100340a006, 1989. 13364, 13387
Huff, A. K. and Thiemens, M. H.: ^{17}O/^{16}O and ^{18}O/^{16}O isotope measurements of atmospheric carbon monoxide and its sources, Geophys. Res. Lett., 25, 3509–3512, doi:10.1029/98GL02603, 1998. 13357, 13368
Johnston, J. C. and Thiemens, M. H.: The isotopic composition of tropospheric ozone in three environments, J. Geophys. Res., 102, 25395–25404, doi:10.1029/97JD02075, 1997. 13357, 13360, 13363, 13367
Kaiser, J., Hastings, M. G., Houlton, B. Z., Rockmann, T., and Sigman, D. M.: Triple Oxygen Isotope Analysis of Nitrate Using the Denitrifier Method and Thermal Decomposition of N_2O, Anal. Chem., 79, 599–607, doi:10.1021/ac061022s, 2007. 13370
Krankowsky, D., Bartecki, F., Klees, G. G., Mauersberger, K., Schellenbach, K., and Stehr, J.: Measurement of heavy isotope enrichment in tropospheric ozone, Geophys. Res. Lett., 22, 1713–1716, doi:10.1029/95GL01436, 1995. 13367
Kunasek, S. A., Alexander, B., Steig, E. J., Hastings, M. G., Gleason, D. J., and Jarvis, J. C.: Measurements and modeling of $\Delta^{17}O$ of nitrate in snowpits from Summit, Greenland, J. Geo-

phys. Res. Atmos., 113, 24302, doi:10.1029/2008JD010103, 2008. 13357, 13359, 13377, 13378, 13380

Lee, C. C. and Thiemens, M. H.: The $\delta^{17}O$ and $\delta^{18}O$ measurements of atmospheric sulfate from a coastal and high alpine region: A mass independent isotopic anomaly, J. Geophys. Res., 106, 17359–17373, 2001. 13357

Luz, B. and Barkan, E.: The isotopic ratios $^{17}O/^{16}O$ and $^{18}O/^{16}O$ in molecular oxygen and their significance in biogeochemistry, Geochimica et Cosmochimica Acta, 69, 1099–1110, doi:10.1016/j.gca.2004.09.001, 2005. 13357

Lyons, J. R.: Transfer of mass-independent fractionation in ozone to other oxygen-containing radicals in the atmosphere, J. Geophys. Res., 28, 3231–3234, doi:10.1029/2000GL012791, 2001. 13360, 13363, 13364, 13380

Mauersberger, K.: Ozone Isotope Measurements in the Stratosphere, Geophys. Res. Lett., 14, 80–83, 1986. 13357

McCabe, J. R., Thiemens, M. H., and Savarino, J.: A record of ozone variability in South Pole Antarctic snow: Role of nitrate oxygen isotopes, J. Geophys. Res. Atmos., 112, 12303, doi:10.1029/2006JD007822, 2007. 13380

Michalski, G., Savarino, J., Bohlke, J. K., and Thiemens, M. H.: Determination of the Total Oxygen Isotopic Composition of Nitrate and the Calibration of a $\Delta^{17}O$ Nitrate Reference Material, Anal. Chem., 74, 4989–4993, 2002. 13362

Michalski, G., Scott, Z., Kabiling, M., and Thiemens, M. H.: First measurements and modeling of $\Delta^{17}O$ in atmospheric nitrate, Geophys. Res. Lett., 30, 14–1, 2003. 13357, 13358, 13359, 13360, 13362, 13363, 13369, 13377, 13380

Morin, S., Savarino, J., Bekki, S., Gong, S., and Bottenheim, J. W.: Signature of Arctic surface ozone depletion events in the isotope anomaly ($\Delta^{17}O$) of atmospheric nitrate, Atmos. Chem. Phys., 7, 1451–1469, 2007a, http://www.atmos-chem-phys.net/7/1451/2007/. 13357, 13359, 13360

Morin, S., Savarino, J., Bekki, S., Gong, S., and Bottenheim, J. W.: Signature of Arctic surface ozone depletion events in the isotope anomaly ($\Delta^{17}O$) of atmospheric nitrate, Atmos. Chem. Phys., 7, 1451–1469, 2007b, http://www.atmos-chem-phys.net/7/1451/2007/. 13363

Morin, S., Savarino, J., Frey, M. M., Yan, N., Bekki, S., Bottenheim, J. W., and Martins, J. M. F.: Tracing the Origin and Fate of NO_x in the Arctic Atmosphere Using Stable Isotopes in Nitrate, Science, 322, 730–732, doi:10.1126/science.1161910, 2008. 13357, 13359

Owens, N. J. P.: Methane flux to the atmosphere from the Arabian Sea, Nature, 354, 293–296, doi:10.1038/354293a0, 1991. 13374

Park, R. J., Jacob, D. J., Field, B. D., Yantosca, R. M., and Chin, M.: Natural and transboundary pollution influences on sulfate-nitrate-ammonium aerosols in the United States: Implications for policy, J. Geophys. Res. Atmos., 109, 15204, doi:10.1029/2003JD004473, 2004. 13359

Patris, N., Cliff, S. S., Quinn, P. K., Kasem, M., and Thiemens, M. H.: Isotopic analysis of aerosol sulfate and nitrate during ITCT-2k2: Determination of different formation pathways as a function of particle size, J. Geophys. Res. Atmos., 112, 23301, doi:10.1029/2005JD006214, 2007. 13357, 13358, 13369

Petit, J. R., Jouzel, J., Raynaud, D., Barkov, N. I., Barnola, J.-M., Basile, I., Bender, M., Chappellaz, J., Davis, M., Delaygue, G., Delmotte, M., Kotlyakov, V. M., Legrand, M., Lipenkov, V. Y., Lorius, C., Pépin, L., Ritz, C., Saltzman, E., and Stievenard, M.: Climate and atmospheric history of the past 420,000 years from the Vostok ice core, Antarctica, Nature, 399, 429–436, doi:10.1038/20859, 1999. 13374

Press, H. W., Teukolsky, A. S., Vetterling, T. W., and Flannery, P. B.: Numerical Recipes in C, Cambridge University Press, 2002. 13365

Rockmann, T., Brenninkmeijer, C. A. M., Saueressig, G., Bergamaschi, P., Crowley, J. N., Fischer, H., and Crutzen, P. J.: Mass-Independent Oxygen Isotope Fractionation in Atmospheric CO as a Result of the Reaction CO+OH, Science, 281, 544, doi:10.1126/science.281.5376.544, 1998. 13357, 13368

Savarino, J. and Thiemens, M. H.: Analytical procedure to determine both $\delta^{18}O$ and $\delta^{17}O$ of H_2O_2 in natural water and first measurements, Atmos. Environ., 33, 3683–3690, doi:10.1016/S1352-2310(99)00122-3, 1999a. 13357, 13377, 13380

Savarino, J. and Thiemens, M. H.: Mass-Independent Oxygen Isotope (16O, 17O, 18O) Fractionation Found in Hx, Ox Reactions, The Journal of Physical Chemistry A, 103, 9221–9229, doi:10.1021/jp991221y, 1999b. 13368, 13377, 13381

Savarino, J., Bhattacharya, S. K., Morin, S., Baroni, M., and Doussin, J.-F.: The $NO + O_3$ reaction: A triple oxygen isotope perspective on the reaction dynamics and atmospheric implications for the transfer of the ozone isotope anomaly, J. Chem. Phys., 128, 194303, doi:10.1063/1.2917581, 2008. 13360, 13364, 13367

Seinfeld, J. H. and Pandis, S. N.: Atmospheric Chemistry and Physics, Wiley-Interscience, 2006. 13362, 13370

Thiemens, M. H.: History and Applications of Mass-Independent Isotope Effects, Ann. Rev.

Earth Planet. Sci., 34, 217–262, 2006. 13357, 13365
Thiemens, M. H. and Heidenreich, J. E.: The mass-independent fractionation of oxygen: A novel isotope effect and its possible cosmochemical applications, Science, 219, 1073–1075, 1983. 13357
Thiemens, M. H., Jackson, T., Mauersberger, K., Schueler, B., and Morton, J.: Oxygen isotope fractionation in stratospheric CO_2, Geophys. Res. Lett., 18, 669–672, 1991. 13357
Yvon, S. A. and Saltzman, E. S.: A Time-Dependent Photochemical Box Model for Atmospheric Chemistry (PBMAC), Ph.D. thesis, University of Miami, Miami, Florida, 1993. 13366
Yvon, S. A., Plane, J. M. C., Nien, C.-F., Cooper, D. J., and Saltzman, E. S.: Interaction between nitrogen and sulfur cycles in the polluted marine boundary layer, J. Geophys. Res., 101, 1379–1386, doi:10.1029/95JD02905, 1996. 13358, 13365, 13366
Zahn, A., Franz, P., Bechtel, C., Grooß, J.-U., and Röckmann, T.: Modelling the budget of middle atmospheric water vapour isotopes, Atmos. Chem. Phys., 6, 2073–2090, 2006, http://www.atmos-chem-phys.net/6/2073/2006/. 13363, 13380

Table 1. Isotopic exchange reactions included in PUB model. References used: a=(Greenblatt and Howard, 1989), b=(Dubey et al., 1997), c=(Dransfeld and Wagner, 1987).

Reaction	k (cm^{-6} s^{-1})	Reference
R13	$1.6\times10^{-13}\exp(-2100/T)$	a
R14	1×10^{-11}	b
R15	$1.7\times10^{-11}\exp(-400/T)$	c

ACPD
9, 13355–13406, 2009

Table 2. Baseline Environmental Variables and their Values.

Variable	Value
Temperature (C)	18.33
Total Ozone Column Density (Dobson Units)	265
Latitude	33
Julian Day	5
Pressure (atm)	1
Altitude of Interest (km)	0
Height of surface above sea-level (km)	0
CH_4 (ppmv)	1.775
CO (ppbv)	60
O_3 (ppbv)	9.3
Alkenes (ppbv)	0.2
Alkanes (ppbv)	0.8
NO (pptv)	50
NO_2 (pptv)	0
Total NO_x (pptv)	0
H_2O (g/kg)	0
H_2O sat vapor pressure (mm Hg)	29.184
Relative Humidity (%)	75
Coarse Aerosol Surface Area ($\mu m^2/cm^3$)	15
Boundary Layer Height (km)	2
DMS Flux(μmole/m^2/day)	20
H_2S Flux (μmole/m^2/day)	0
NO Flux (μmole/m^2/day)	0
Integration Stop Time (hours)	150
Cloud Base Height (km)	5
Cloud Albedo	0.01
Surface Albedo (only for fixed albedo runs)	0.07
DMS Branching Ratio (fraction of DMS going to SO_2)	0.96
Fine Aerosol Surface Area ($\mu m^2/cm^3$)	15
$\gamma(HNO_3)$	0.10
$\gamma(N_2O_5)$	0.05

Table 3. Oxygen bearing trace species and their $\Delta^{17}O$ values.

Trace Species	$\Delta^{17}O$(‰) range
CH_3O	[0–25]
CH_3O_2	[13–27]
CH_3O_2H	[1–22]
HCHO	[2–15]
CHO	[0–15]
PAN	[18–31]
HNO_2	[19–31]
CH_3CO_3	[19–31]

Table 4. Summary of Environmental Sensitivities of $\Delta^{17}O(NO_3^-)$. Sensitivities for precursors of aerosol nitrate also follow similar trends and offsets.

Variable (units)	Range	$\Delta^{17}O(NO_3^-*)$‰
Ozone Column (DU)	[200–500]	[20.1–26.1]
Boundary Layer Height(km)	[0.5–3]	[29.9–21.1]
Cloud Base Height (km)	[2–6]	[22.2–21.4]
DMS Flux(μmoles $m^{-2}dy^{-1}$)	[0–50]	[19.0–24.3]
H_2S Flux (μmoles $m^{-2}dy^{-1}$)	[0–30]	[21.4–23.8]
Julian Day	[0–185]	[21.5–17.1]

Table 5. Sources of HO_2 in Model and Significance. Production % estimates based on typical model outputs for [OH], [O_3], [H].

Reaction	$k(T=298\ \mathrm{K})\ \mathrm{cm}^{-6}\ \mathrm{s}^{-1}$	Production % Range
R17	1.06×10^{-11}	~0.99–0%
R18	6.82×10^{-14}	$\ll$1%
R19	1.69×10^{-12}	$\ll$1%
R20	0.23	~0–0.99%

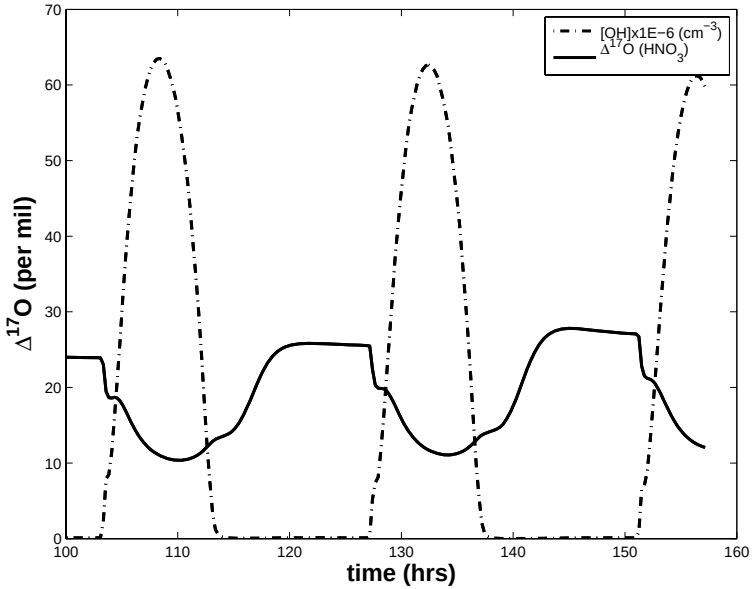

Fig. 1. Diurnal variation of [OH] and $\Delta^{17}O$ of HNO_3 typically seen in model output. Output shown for $[O_3]$=1 ppm and baseline values for other variables.

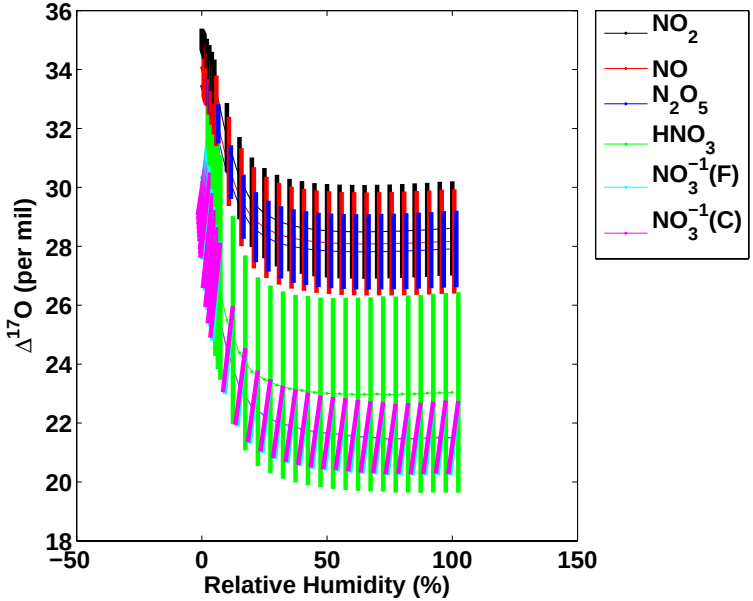

Fig. 2. Sensitivity of $\Delta^{17}O$ to Relative Humidity.

ACPD
9, 13355–13406, 2009

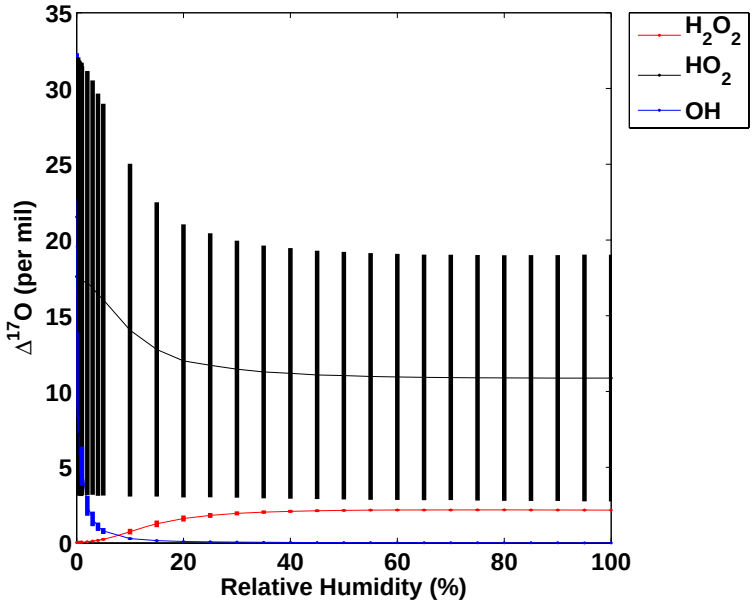

Fig. 3. Sensitivity of $\Delta^{17}O$ of HO_x and H_2O_2 to Relative Humidity. We note that in the limit of 0% RH, the $\Delta^{17}O$ of OH converges to 26‰.

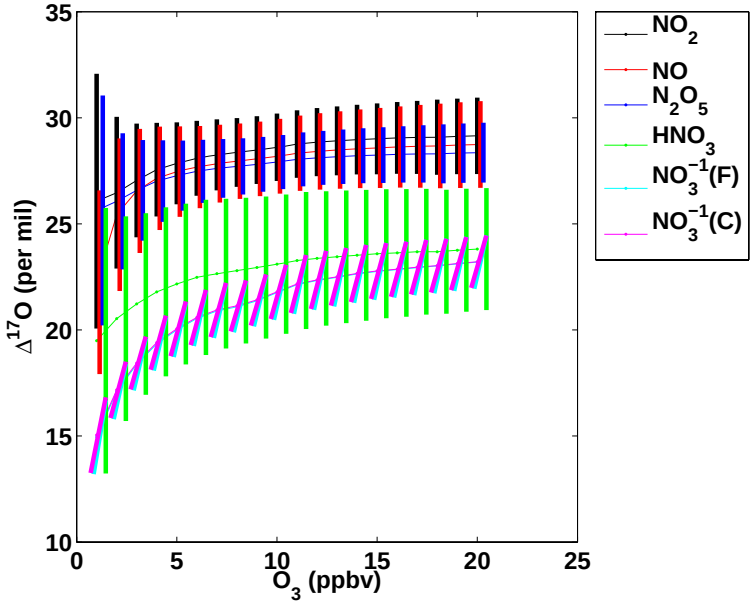

Fig. 4. Sensitivity of Δ^{17}O to O_3.

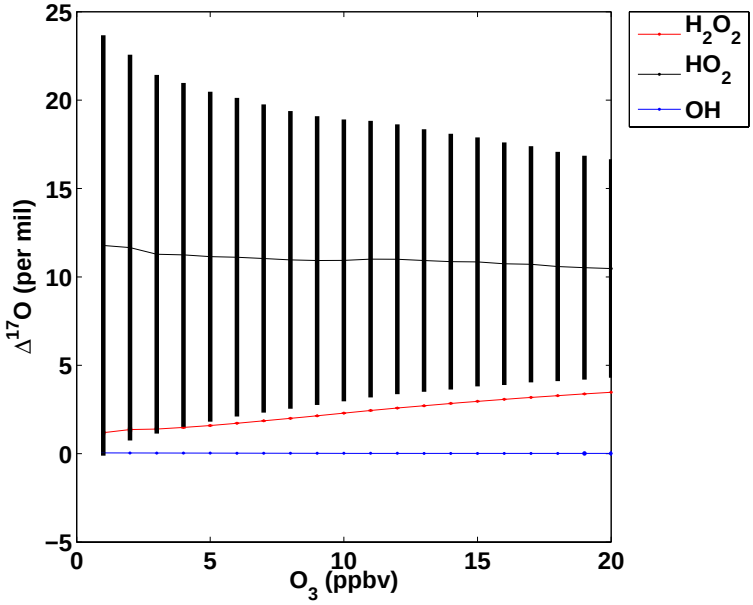

Fig. 5. Sensitivity of Δ^{17}O of HO_x and H_2O_2 to $[O_3]$.

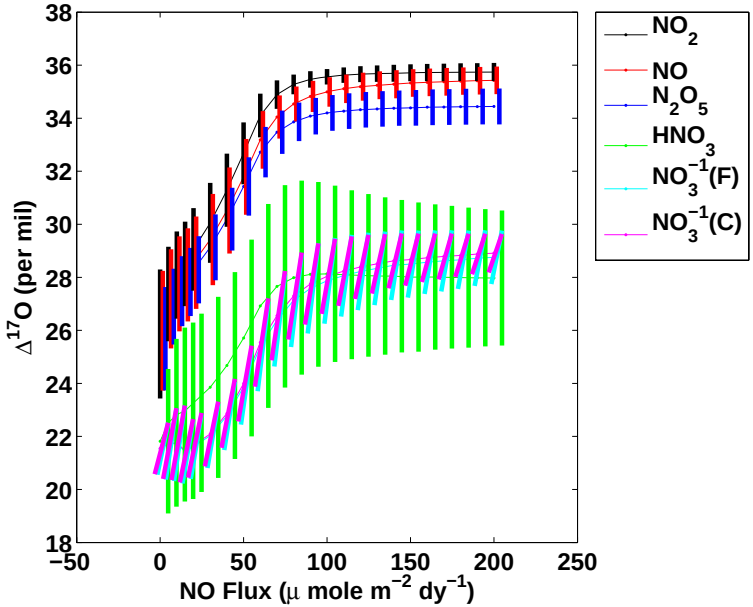

Fig. 6. Sensitivity of $\Delta^{17}O$ to NO_x flux.

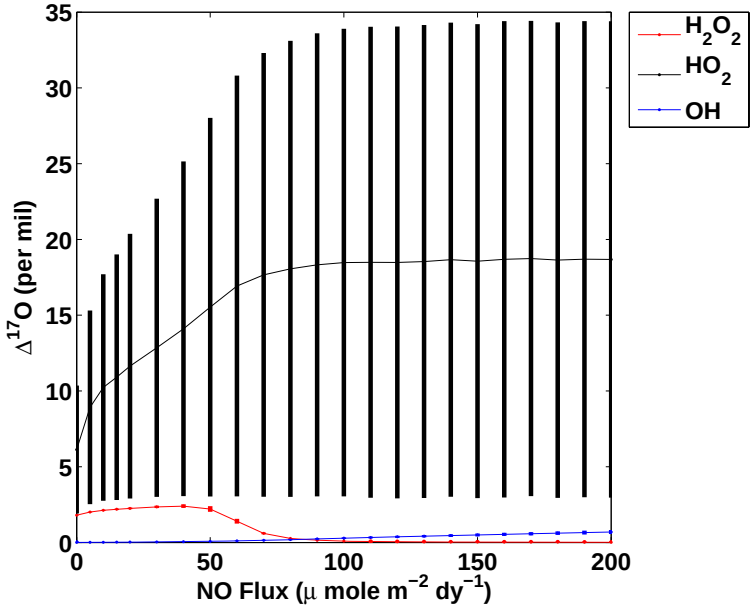

Fig. 7. Sensitivity of $\Delta^{17}O$ of HO_x and H_2O_2 to NO_x flux.

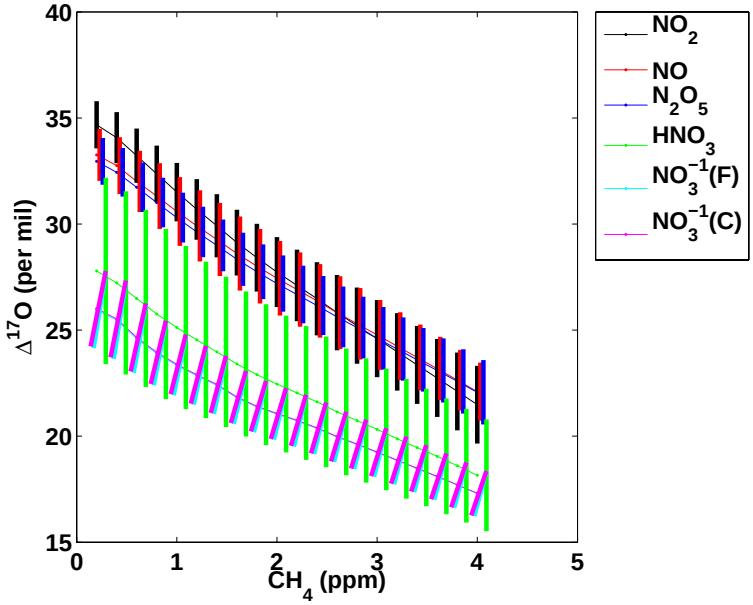

Fig. 8. Sensitivity of $\Delta^{17}O$ to $[CH_4]$.

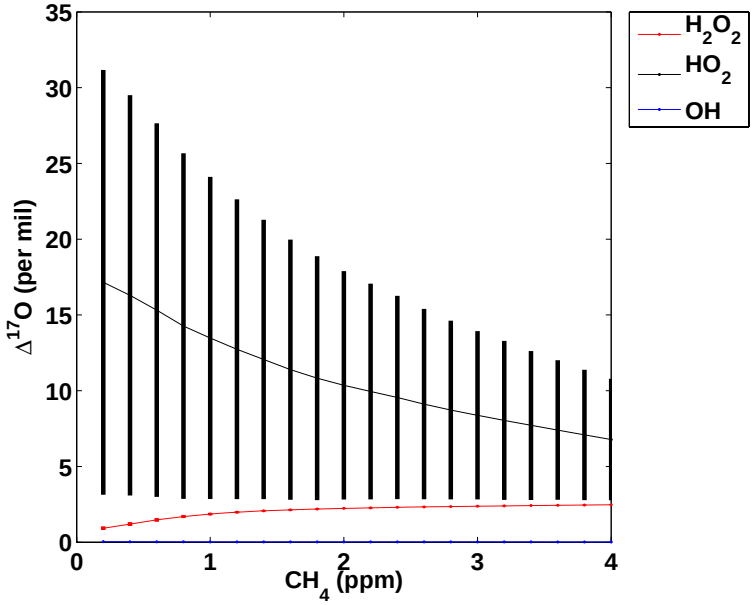

Fig. 9. Sensitivity of Δ^{17}O of HO_x and H_2O_2 to CH_4 concentration.

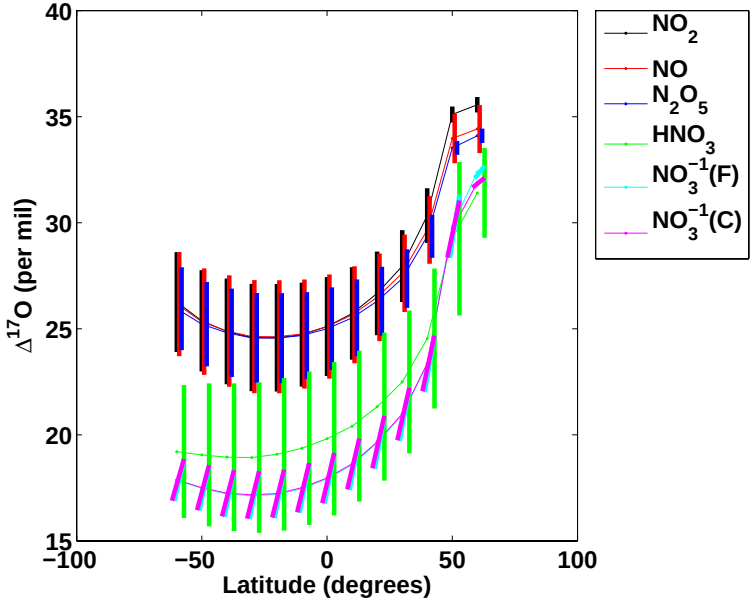

Fig. 10. Sensitivity of $\Delta^{17}O$ to Latitude.

ACPD
9, 13355–13406, 2009

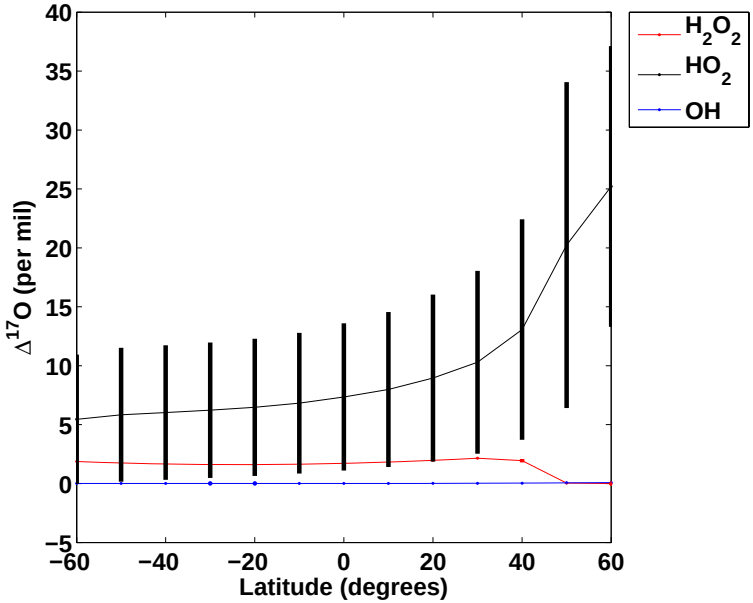

Fig. 11. Sensitivity of $\Delta^{17}O$ of HO_x and H_2O_2 to Latitude.

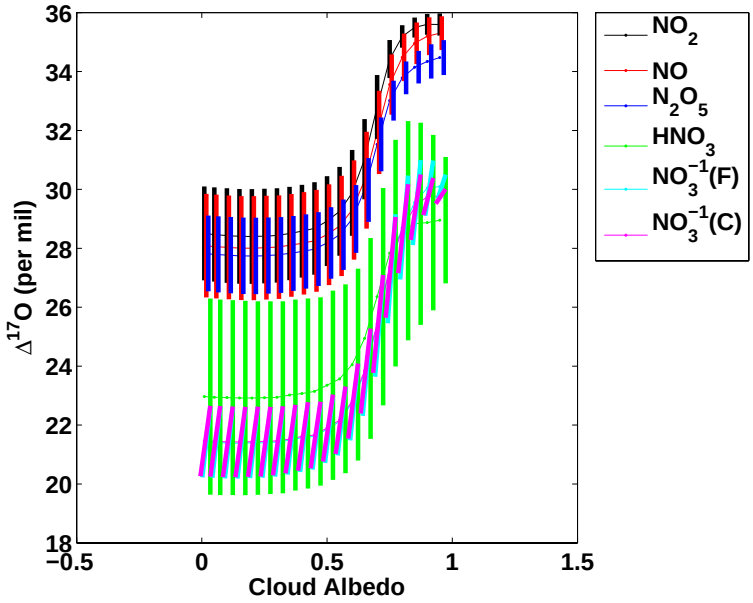

Fig. 12. Sensitivity of $\Delta^{17}O$ to Cloud Albedo.

ACPD
9, 13355–13406, 2009

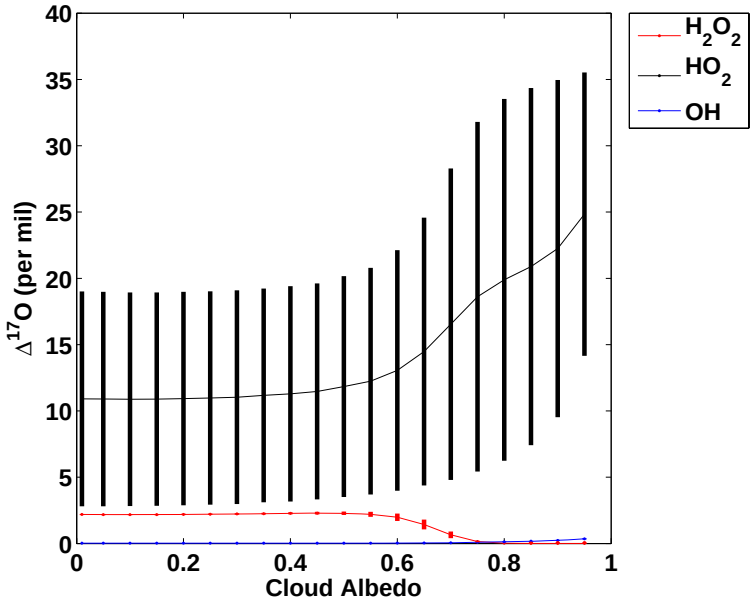

Fig. 13. Sensitivity of $\Delta^{17}O$ of HO_x and H_2O_2 to Cloud Albedo.

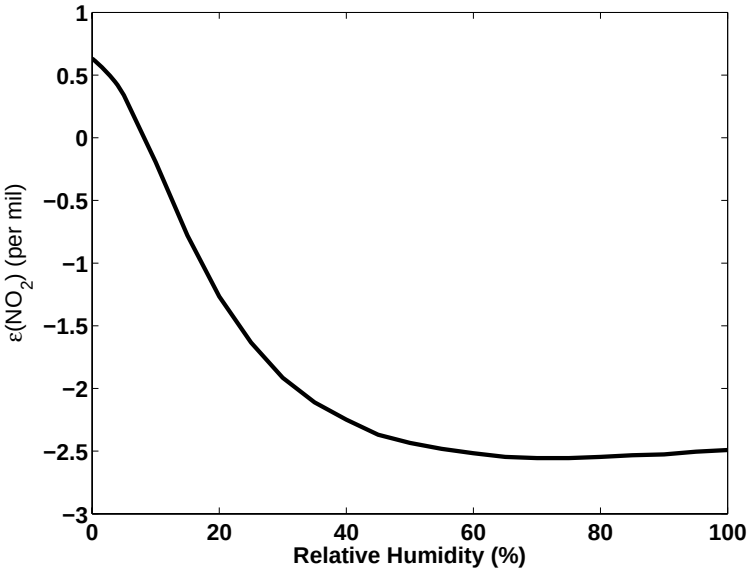

Fig. 14. Error in $\Delta^{17}O(NO_2)$ as a function of Relative Humidity. The large differences at low relative humidity are contributed in part by the fact that the $\Delta^{17}O$ (OH) becomes significantly greater than 0 at very low humidities.

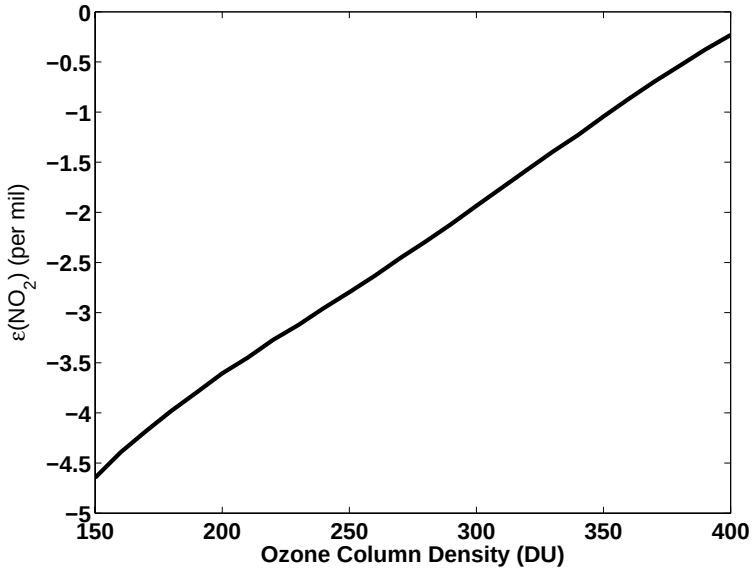

Fig. 15. Error in $\Delta^{17}O(NO_2)$ as a function of total ozone column density.